T-CYCLE EPR Development at 275 GHz for the study of reaction kinetics & intermediates

Panarelli, E.G.

2

Effective coupling of Rapid Freeze-Quench to High-Frequency Electron Paramagnetic Resonance

2.1 Introduction

Determination of reaction rates and detection of short-lived intermediates of fast chemical reactions are an important goal in those fields that involve molecular chemistry, such as biochemistry, pharmaceutics, medicine, environmental science, and material science, to name a few. Kinetics and intermediates shed light on the mechanism of a reaction, which in turn yields broader information about the chemical system under study.

One possible stratagem to investigate chemical kinetics is that of letting the reaction unfold for controlled time steps and then "freezing" it. In this way it is possible to follow the decay and growth of reactants and products, or the evolution of reaction intermediates. One of the most widely used techniques to attain this is called *Rapid Freeze-Quench* (RFQ), in use since 1961 [18], which is often coupled to Electron Paramagnetic Resonance (EPR) in view of the paramagnetic nature of the intermediates of a great deal of chemical reactions.

The multi-frequency approach in EPR is of particular interest, namely when low-frequency experiments (e.g. those at the standard frequency of 9.5 GHz, called X-band) are combined with high-frequency ones (HF-EPR, e.g. those at microwave frequencies of 95 and 275 GHz). Such approach offers a better and more complete characterization of the magnetic system under study. However, collection of RFQ samples is – to say the least – problematic for applications in HF-EPR, because the size of HF resonant cavities is hugely reduced as compared to the standard 9.5 GHz EPR, thus making the sample holders and the sample volume dramatically small. In Table 2.1 is shown a comparison of the typical sample volumes used for three EPR frequencies, namely 9.5, 95, and 275 GHz. The sample volume downsizes by about 10^4 times going from low to high frequency. It is therefore vital to develop a sample packing technique that guarantees an efficient, homogeneous, and reproducible sample collection in the small capillaries used as sample holders for HF-EPR.

Frequency (GHz)	Cavity length (mm)	Effective sample volume
9.5	30	100 μL
95	4	1 μL
275	1	20 nL

Table 2.1: Comparison of the sample volumes involved in some EPR frequencies.

In the literature there have been endeavors to implement and standardize packing techniques for RFQ-EPR applications [35] [36] [37] [38] [39] [40] [21].

Ballou *et al.* [35] and Oellerich *et al.* [36] are the earliest reported attempts to study a chemical reaction detected with X-band EPR on a timescale of less than 80 ms. Although of great interest given the short timescale, both authors attribute the large inaccuracy on the reaction rates (errors bigger than 10%) to the nonuniform and irreproducible packing of the RFQ particles. Indeed, in both papers the authors report a rather low and nonhomogeneous packing efficiency, between $0.5 \div 0.7$ the former, and between $0.4 \div 0.6$ the latter. Oellerich even concludes that this problem constitutes an "intrinsic deficiency of freeze-quench EPR spectroscopy", and indeed, as described below, this is a serious issue not easily circumvented.

Nami *et al.* [37] propose an improved method to collect and pack RFQ particles from an isopentane suspension, based on pumping said suspension through an EPR tube in which a filter has been placed. The RFQ particles are trapped at the filter and the isopentane is easily removed. The advantages of this method are its reproducibility and efficiency: the authors report a packing factor between $0.68 \div 0.76$, which is indeed a considerable improvement, also compared to previous studies (see below). A slightly modified version of this method is applied in this work.

Schuenemann *et al.* [38] are the first to report the application of RFQ to HF-EPR in a multi-frequency EPR study (at 9.6, 94, 190, and 285 GHz), on a timescale of up to 40 ms. Although HF-EPR implies dealing with sample holders of reduced size, the method used by the authors to pack the RFQ for HF-EPR is basically the same as for low frequency, i.e., compacting the sample sprayed in a tube of the appropriate size by means of a metal rod. However, the authors' focus is to detect the reaction intermediate of the reaction under study, rather than its reaction rate, so that inhomogeneous sample packing is of no concern to them.

In the context of RFQ-HFEPR, Manzerova *et al.* [39] bring about an innovative method to freeze-quench reactants, reduce them to fine particles, and collect them. They report a technology based on rotating copper wheels kept at a temperature of 80 K, on which the mixture of the reactants is sprayed through a home-built nozzle. The reactant mixture is thus freeze-quenched, and the sample is then "scraped" off the wheels and collected by tapping with a capillary suitable for 130 GHz EPR. Although such approach introduces the advantage of not having to handle static frozen particles floating in isopentane, the packing factor the authors report is 0.5, thus being no improvement as compared to those from the aforementioned studies.

All of the aforesaid publications require a large amount of sample, which is often a disadvantage when working with biological samples. Kaufmann *et al.* [40] and Pievo *et al.* [21] reported the development of, respectively, a micro-fluidic mixer (after its introduction by Cherepanov and de Vries [20]) and a micro-mixer, both requiring volumes of hundreds of microliters, thus suitable

for RFQ-HFEPR studies of biological samples. It is interesting that Kaufmann also implemented a new way of collecting the RFQ samples, based on the idea of Manzerova [39]: they use a rotating aluminum plate kept at a temperature of 80 K, on which the reagent mixture is sprayed and freeze-quenched. The RFQ powder is then collected by tapping the capillary on it. However, the packing efficiency is not mentioned, while in [21] a packing factor of $0.5 \div 0.6$ is reported. From the cited literature thus emerges a serious difficulty in RFQ-HFEPR when it comes to collect RFQ particles and study them in a standardized, efficient, and reproducible way.

In the literature, a common and practical way of testing the performance of RFQ-HFEPR is making use of the binding reaction of sodium azide to myoglobin. This reaction (Scheme 2.1) is a well-understood model system that offers several advantages in EPR studies because of its convenient spectral properties [35] [36] [21].

$$[\mathrm{Fe}^{3+}_{HS}\text{—}\mathrm{OH}_2] + \mathrm{N}_3^- \rightarrow [\mathrm{Fe}^{3+}_{LS}\text{—}\mathrm{N}_3^-] + \mathrm{H}_2\mathrm{O} \tag{2.1}$$

Myoglobin (abbreviated Mb) is an iron- and oxygen-binding hemoprotein, similar to hemoglobin, whose function is that of reversibly storing and transporting oxygen in the muscle tissues of many vertebrates [41]. At neutral pH, the heme iron (Fe(III), a d^5 ion) of ferric myoglobin (also known as *met-myoglobin*) exhibits an octahedral coordination environment with one of the axial positions being occupied by variable ligands. The nature of such variable ligands determines the energy splitting between the upper and lower groups of d orbitals. Water can be one of these ligands, and weakly binding to the heme-Fe(III), thus generating a high-spin (HS) $S = {}^5\!/_2$ state. However, when an exogenous strong-binding ligand such as azide (N_3^-) replaces the axial water molecule, the stronger ligand-field effect induced on Fe(III) converts its spin state to low-spin (LS) with $S = {}^1\!/_2$. Scheme 2.1 illustrates the binding reaction of azide to myoglobin.
The spectral features of HS- and LS-Fe(III) are completely different, the former having an intense signal around $g = 6$, while the latter having a rhombic signal around $g = 2$. Such features turn out to be so handy that the binding reaction of sodium azide to myoglobin has become a standard when evaluating RFQ-EPR methods, both at low and high frequency [35] [36] [39] [21].

The present work originates from the premises cast by Nami in her PhD thesis [42], who explored the feasibility of multi-frequency EPR coupled with RFQ making use of the binding reaction of sodium azide to met-myoglobin, based on an improved method to pack and load capillaries for HF-EPR [37]. However, her investigations at high-frequency EPR (95 and 275 GHz) yielded unconvincing results, given the huge scatter of the data points. The two main limitations that can be envisaged in [42] are:

- The reaction time scale selected for the study was very short, namely less than 10 ms for a reaction with a characteristic time twice as long;
- The manganese(II) ions introduced in the RFQ samples, used for internal calibration, were originally mixed in the sodium azide solution, rather than in the myoglobin solution. In this way, the $^{Mb}/_{Mn^{2+}}$ ratio is affected by possible irreproducible mixing of the RFQ apparatus, which results in an inconstant ratio for different RFQ samples.

For these two reasons, in this work it was chosen to select a longer time scale for the myoglobin reaction of Scheme 2.1 (namely, up to $\sim$ 50 ms), and to add $MnCl_2$ to the myoglobin solution, rather than to the sodium azide solution, prior to mixing in the RFQ apparatus.

Another critical aspect of this study is the packing of the RFQ samples in the sample holders suitable for 275 GHz EPR, namely quartz capillaries with an inner diameter of 150 μm, hosting a sample volume of 20 nL in the resonant cavity. While the general procedure to prepare the X-band RFQ samples is the same as described in [42], an improved method for sample preparation for 275 GHz was devised.

2.2 Experimental

2.2.1 Materials

Equine-heart met-myoglobin, sodium azide (NaN_3), and DMSO were purchased from Sigma-Aldrich (cat. n. M1882-1G, 15,795-3, and 154938-1L respectively). $MnCl_2$ was purchased from Baker Chemicals (cat. n. 0173). Myoglobin was dissolved in phosphate buffer 100 mM at pH 7.8, with the addition of 5% v/v DMSO and 50 μM of $MnCl_2$, to form a solution with concentration 2.4 mM. Sodium azide was dissolved in phosphate buffer 100 mM at pH 7.8 to form a solution with concentration 24 mM. After RFQ mixing, the Mb:azide ratio is 1.2:12 mM. The concentration of the myoglobin solution was determined spectrophotometrically using the extinction coefficient $\epsilon_{505} = 9.7$ mM^{-1} cm^{-1}.

2.2.2 Sample preparation

Ten RFQ samples (named Mb1 to Mb10) were prepared with the same RFQ apparatus and method described in [37] (2-mL syringes, ram velocity 3.2 cm s^{-1}, displacement 3 mm), at a mixing temperature of 21.5 °C, and at reaction times ranging between 2 and $\sim$ 50 ms. These

ten samples were initially measured at 9.5 GHz, and later (about a year after), the same were used for measurements at 275 GHz.
Table 2.2 summarizes, for each RFQ sample, the corresponding reaction time, that is calculated from the parameters used in the RFQ setup, and not corrected by the so-called *freezing time*.

RFQ sample label	Mb1	Mb2	Mb3	Mb4	Mb5	Mb6	Mb7	Mb8	Mb9	Mb10
Calculated reaction time (ms)	2.0	3.1	4.9	7.8	9.8	15.6	25.0	31.3	39.1	48.8

Table 2.2: Calculated reaction time of the RFQ samples.

In addition, two myoglobin solutions without any sodium azide were prepared (labeled Mb0), meant to represent reaction 2.1 before it has started, namely at $t = 0$. For the spectra at 9.5 GHz, the Mb0 solution was prepared from the same batch used to prepare the RFQ samples. However, for the spectra at 275 GHz, since about a year passed from the preparation of the RFQ samples, the Mb0 solution was made from an independent batch, but with identical composition as described in Subsection 2.2.1.

Sample packing for 9.5 GHz EPR

The preparation of RFQ samples for 9.5 GHz EPR is a procedure that was successfully standardized by Nami [37]. With this procedure, the RFQ samples are straightforwardly packed in quartz tubes, readily used as sample holders for 9.5 GHz EPR. The essential steps of this procedure, conducted in a polystyrene box filled with dry ice pellets, are briefly reported below:

- The quartz tubes (10 cm long, 3 mm inner diameter) are open on both sides, and are customized by tapering them on one side. This allows the accommodation of a polypropylene disk used as a filter.

- The tapered end is connected through a latex tubing to a hand-held 60-mL Norm-Jet disposable syringe used to create underpressure (instead of a water aspirator, as described in the original procedure).

- While manually creating underpressure in the syringe, the other side of the quartz tube is dipped in cold isopentane contained in a vial in contact with dry ice. The isopentane is thus aspirated through the tube, which is pre-cooled by it.

- By maintaining the underpressure in the syringe, the pre-cooled quartz tube is quickly transferred into the vial containing the RFQ sample in cold isopentane. This vial has previously been lain on dry ice to ensure thermal contact. By pushing the quartz tube to the end of the sample vial (and making sure that the filter-containing tapered part is always in contact with dry ice so as to prevent the sample from warming), the RFQ sample is sucked up the tube and accumulates through it thanks to the filter. With the settings of the RFQ apparatus described above, a 3-mm quartz tube is typically filled with roughly 4 to 5 cm of sample.

- When all the isopentane contained in the sample vial has been aspirated, the latex tubing is cut and the quartz tube is stored in liquid nitrogen. As opposed to the procedure described in [42], the sample in the tube is not further packed more tightly with a steel rod because of the relatively big amount of sample present in the tube, and because a tighter packing would result in a more difficult handling for applications at 275 GHz (see 2.2.2).

The quartz tubes prepared in this way are ready to be measured with a 9.5 GHz EPR spectrometer, and do not need further treatments.

Sample packing for 275 GHz EPR

The preparation of RFQ samples for 275 GHz EPR is by far more complicated than for 9.5 GHz EPR. The minuscule size of the capillaries used as sample holders (150 μm inner diameter) poses a twofold problem. Firstly, accidental warming of the samples is easy and fast, in view of the tiny volumes involved. For this reason, since the warming of the samples has to be avoided at all costs, they have to be handled at cryogenic temperatures. This leads to the second issue, which is the difficulty of handling such small capillaries in a cryogenic atmosphere, while wearing cryoprotective gloves that reduce the user's hand sensibility.
A successful sample packing in capillaries for 275 GHz EPR is thus a troublesome procedure that requires a trained operator. Following is a description of the basic steps of this procedure (as reported in essence in [42]), which is carried out in a polystyrene box half-filled with liquid nitrogen. Thanks to a flow of cold nitrogen gas blowing on the surface of the liquid nitrogen, the average temperature in the box within the first 10 cm from the liquid nitrogen surface is kept below -100 °C.

- A home-built stainless-steel plate (15 $\times$ 15 cm) is placed on top of an octagonal polystyrene box (14 $\times$ 14 $\times$ 6 cm). The plate has a central hole (6 cm diameter) that accommodates an agate mortar (whose surface sits at the same height as the plate), tightened with screws. This mortar is used to grind the RFQ samples under liquid nitrogen. The plate

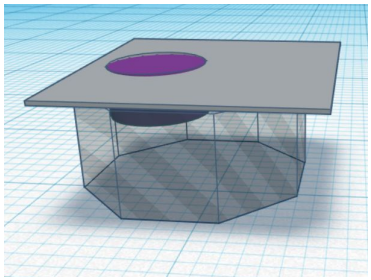

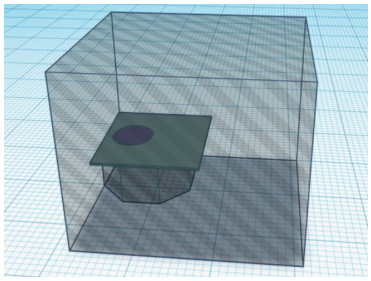

Figure 2.1: 3D renderings of the tools used for the packing procedure for 275 GHz EPR. Left: octagonal polystyrene box with metal plate and agate mortar on top. Right: bigger polystyrene box to be filled with liquid nitrogen. (This rendering does not show the grid-like array of holes perforated on the metal plate.)

also features a grid-like array of perforated holes (2 mm diameter, separated by 1 cm), which allow a better thermal exchange with the liquid nitrogen beneath once the box is filled.

- The ensemble of plate, mortar, and octagonal box (Figure 2.1, left) is placed in another, larger polystyrene box (29 × 25 × 24 cm), which is then filled with liquid nitrogen up to the level of the plate surface (Figure 2.1, right). In this way, also the octagonal box will fill with liquid nitrogen, and so will the mortar, which will always be immersed in it. It is important, prior to pouring the nitrogen, to wet the outside bottom of the octagonal box, so that a film of ice will form that keeps the octagonal box steady in its position during the procedure.

- A RFQ sample contained in a quartz tube (as described in 2.2.2) is transferred from liquid nitrogen into dry ice pellets for a few minutes to ensure the softening of the content upon reaching a relatively higher temperature. In this way, after quickly transferring the quartz tube onto the plate contained in the liquid nitrogen box, it is possible to collect the RFQ sample in the form of pellets by tapping the surface with a pre-cooled glass capillary (2 mm outer diameter). This pellet of sample is then dropped in the mortar filled with liquid nitrogen with the help of another, smaller pre-cooled glass capillary (1.1 mm outer diameter) pushed through the first one. Two to four pellets are the necessary amount of sample to be ground and packed in a capillary for 275 GHz EPR.

- The pellets of sample are ground to a fine powder in the mortar filled with liquid nitrogen,

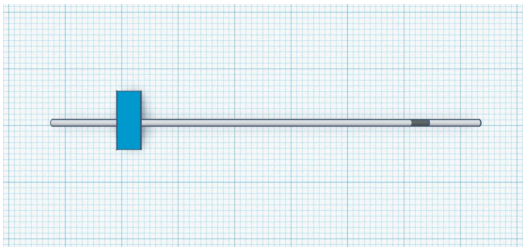

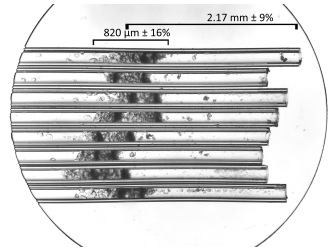

Figure 2.2: Customized quartz capillaries for the 275 GHz EPR packing procedure. Left: simplified model of a customized quartz capillary. For the sake of a visually better representation, the capillary in the scheme is not in scale. Right: microscope magnification of eight quartz capillaries. Only the end of the capillaries containing the filter is shown, with average values of suitable filter thickness and filter distance from the capillary end.

by means of a pre-cooled agate pestle. Since the ground sample has the tendency to stick onto the surface of the mortar, it is important to scoop it with a pre-cooled metal spatula so as to stir it around and facilitate the packing procedure.

- A customized quartz capillary of 150 μm inner diameter is used to collect the sample (Figure 2.2, left). Note that the customized capillary has a small tape flag that ensures the filter (and therefore the sample) to sit at a fixed position in the capillary, so that the sample will result in the middle of the insert's resonant cavity. Also, it can be noticed that the capillary has an extra portion of it beyond the flag. This portion allows the capillary to be connected - through a plastic tubing - to a 60-mL Norm-Jet disposable syringe with a straight-cut Luer needle, used to manually create underpressure over the capillary and aspirate the powdered sample.

- Once the capillary is connected to the syringe, the underpressure made, and the capillary pre-cooled, the latter is dipped into the mortar, and by manually keeping the syringe piston tight, the sample is sucked up the capillary till the silica gel filter, where it accumulates. This is a critical step, because if the filter does not have specific value ranges of thickness and distance from the capillary bottom (Figure 2.2, right), the powdered sample will accumulate only at the tip of the capillary and get stuck there. This results in a gradual decrease of the underpressure, and further packing is made impossible.

- When at least 5 mm of the capillary have been filled with sample, the capillary is placed

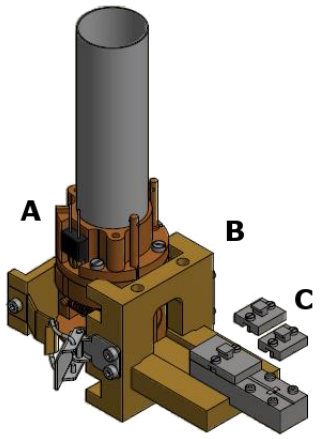

Figure 2.3: 3D rendering of the home-built probe head used for 275 GHz EPR (A), the loading stage clamped to the probe head (B), and the metal block with its three lids used to keep the sample cold (C).

on a pre-cooled home-built metal block (Figure 2.3, C), whose function is that of helping keep the capillary at low temperature, protecting it from accidental warming. The extra portion of capillary connected to the syringe is cut, and the metal block is closed with its own lids, which are then fixed with screws. The metal block is then put in dry ice, and is ready for the loading. At least two to three capillaries are prepared per sample, because their accidental breaking or exposure to room temperature is easy during handling and loading.

Sample loading for 275 GHz EPR

As opposed to the straightforward sample loading for 9.5 GHz EPR, at 275 GHz special care and equipment is needed for the reasons exposed in 2.2.2.
Ensuring that the sample stays at cryogenic temperature during the whole loading procedure is paramount. To this end, at the moment of the sample loading the spectrometer probe head has to be pre-cooled to a temperature between -90 and -80 °C (i.e., about the temperature of dry ice). With the help of a loading stage that can be clamped to the probe head (Figure 2.3, B), a capillary can be transferred from the metal block where it is accommodated (Figure 2.3, C) into the probe head. Also the loading stage is pre-cooled to dry-ice temperature, and the loading procedure is carried out under a flow of cold nitrogen gas that prevents excessive warming of the

components and of the sample, and prevents from excessive water condensation from air.
Once the loading stage is clamped onto the probe head and the metal block is correctly positioned on the loading stage, the transfer of the capillary is done by lifting up the block's lid that lies farthest away from the probe head entrance (i.e., the region of the capillary where the RFQ sample sits), and simply pushing the capillary towards the probe head. This action is repeated two more times, i.e., until the last lid (the one lying closest to the probe head) has been lifted, and the whole capillary is located inside the probe head. Afterwards, the probe head can be put back into the cryostat and taken to the desired temperature.
In this way the sample is never exposed to warm air, and stays at cryogenic temperature from the beginning to the end of the loading procedure.

2.2.3 EPR measurements

EPR measurements were performed with a 9.5 GHz (X-band) and a 275 GHz spectrometer. The former is an ELEXSYS E680 X-band (9.5 GHz) spectrometer from Bruker BioSpin GmbH, equipped with a He-flow ESR900 cryostat from Oxford Instruments. The latter is a home-built spectrometer [34], equipped with a He-flow CF935 cryostat from Oxford Instruments, and a home-built probe head with a single-mode cavity specifically designed for cw measurements [43]. The 275 GHz EPR spectrometer operates with a 14-Tesla superconducting magnet having a IPS120-10 power supply, both from Oxford Instruments, which allow a precision on the magnetic field of less than 0.01 mT.
The experimental parameters used to record the EPR spectra of the RFQ samples are summarized in Table 2.3. The X-band spectra were recorded averaging 4 scans at a temperature of 20 K, and within a field range of less than 500 mT it is possible to detect both the HS-Fe(III) (low field), and the LS-Fe(III) (high field). The 275 GHz spectra were recorded averaging between 16 to 36 scans (depending on the sample) at a temperature of 10 K, and, given the high magnetic field required to operate at such high frequency, it is not convenient to record both the low-field HS-Fe(III) signal and the high-field Mn^{2+} one in one single spectrum. Whenever shown, error bars represent the noise level of the averaged spectra.

2.2.4 Internal calibration

RFQ samples are inherently heterogeneous because of both the quality of the mixing, and the amount and density of the packed particles in the collection tubes. In order to achieve quantitative results it is therefore pivotal to device a way to calibrate the EPR signals resulting from such samples. For low-frequency 9.5 GHz EPR (X-band), this is readily attained, because both the

EPR freq. (GHz)	Field range (mT)	# of points	Mod. freq. (kHz)	Mod. ampl. (mT)	Time const. (s)	Conversion time (ms)	Microwave power (μW)	T (K)
9.5	2.5 ÷ 447.5	4096	100	0.5	0.08	40.96	100	20
275 (Mb part)	3100 ÷ 4000	1000	1.7	1.3	3	250	1.74	10
275 (Mn part)	9810 ÷ 9885	1000	1.7	0.3	1	500	0.83	10

Table 2.3: Experimental parameters of the spectra at 9.5 GHz and 275 GHz. *Mod. freq.* and *Mod. ampl.* are the field modulation frequency and amplitude, respectively.

low-field HS-Fe(III) and the high-field LS-Fe(III) are detectable, and the total intensity of the heme-Fe(III) is distributed between these two forms [21]. However, since at high-frequency 275 GHz EPR only the low-field HS-Fe(III) is visible, a reference signal is needed to normalize the Fe(III) signal. This is achieved by addition of $MnCl_2$ to the myoglobin solution [44], prior to the mixing in the RFQ apparatus. The Mn^{2+} ion exhibits intense, sharp peaks around $g = 2$, a feature that makes it ideal for use as an internal standard.

2.2.5 Methodology

The myoglobin-to-azide ratio of 1:10 allows to treat reaction 2.1 as a pseudo-first-order kinetics [42], so that the logarithmic ratio of the concentration of the HS-Fe(III) at any reaction time t and at time $t = 0$ (from now on, $[HS]_t$ and $[HS]_0$, respectively) is proportional to the reaction time (Equation 2.2). The k' is called the *apparent* reaction rate, and is the product of the actual reaction rate and the azide concentration, $[N_3^-]$ (Equation 2.3).

$$\ln \frac{[HS]_t}{[HS]_0} = -k' \cdot t \tag{2.2}$$

$$k' = k \cdot [N_3^-] \tag{2.3}$$

At high-frequency EPR (275 GHz), the ratio of the HS-Fe(III) concentrations, $[HS]_t/[HS]_0$ (from now on defined as $Y(t)$), is directly proportional to the ratio of the EPR intensity of the respective signals normalized by the Mn^{2+} signal, $(S'_{HS})_t/(S'_{HS})_0$, as shown in Equation 2.4. Note that S' represents the signal S *normalized* by manganese (Equation 2.5).

$$Y(t) = \frac{[HS]_t}{[HS]_0} = \frac{(S'_{HS})_t}{(S'_{HS})_0} \tag{2.4}$$

$$(S'_{HS})_t = \frac{(S_{HS})_t}{S_{Mn}} \tag{2.5}$$

At 9.5 GHz, the detection of Mn^{2+} is problematic, so that the normalization of the HS-Fe(III) signal is done with the LS-Fe(III) one (S_{LS}). Pievo *et al.* [21] showed that in this case $Y(t)$ can be written as:

$$Y(t) = \frac{R_t}{R_t + \lambda} \tag{2.6}$$

$$R_t = \frac{(S_{HS})_t}{(S_{LS})_t} \tag{2.7}$$

$$\lambda = \frac{(S_{HS})_0}{(S_{LS})_\infty} \tag{2.8}$$

where the λ factor in Equation 2.6 is the ratio of the HS-Fe(III) signal at $t = 0$, $(S_{HS})_0$, (i.e., reaction not begun yet), and the LS-Fe(III) signal at $t \to \infty$, $(S_{LS})_\infty$, (i.e., reaction completed), as expressed in Equation 2.8. R_t is the ratio of the HS- and LS-Fe(III) at the time t.

Both at 9.5 GHz and at 275 GHz, the signals S used in Equations 2.2 to 2.8 were the peak-to-peak intensities of the spectra of Figure 2.4 (at 9.5 GHz) and Figure 2.7 (at 275 GHz), measured at appropriate field values.

2.3 Results

The X-band spectra of the ten myoglobin-azide RFQ samples in the time range between 2.0 and 48.8 ms show a clear decay of the low-field HS-Fe(III) signal at $B_0 = 115.3$ mT, accompanied by a proportional increase of the rhombic high-field LS-Fe(III) one at $B_0 =$ 241.9, 304.8, and 391.9 mT (Figure 2.4). It can be noticed that already in the Mb1 sample at $t =$ 2.0 ms the LS-Fe(III) is detectable, while in the Mb10 sample at $t =$ 48.8 ms the HS-Fe(III) signal has not completely disappeared, indicating that the reaction is not completed yet.

Figure 2.5 (top) shows the signal decay $Y(t)$ obtained from the X-band spectra, versus the calculated reaction time (see Table 2.2). The HS signal intensity was taken at $B_0 =$ 112.7 mT (max) and $B_0 =$ 117.2 mT (min), while the LS signal intensity was taken from the central component of the rhombic spectrum at $B_0 =$ 304.0 mT (max) and $B_0 =$ 306.3 mT (min). Spectra of RFQ samples Mb5, Mb6, Mb8, and, to a lesser extent, Mb10, show a broadened signal in the range B_0 between 150 and 250 mT, clearly due to a contamination most likely during the preparation of the RFQ samples. However, this contamination does not prevent an accurate determination of the intensity of the signals of interest, since they fall outside of the

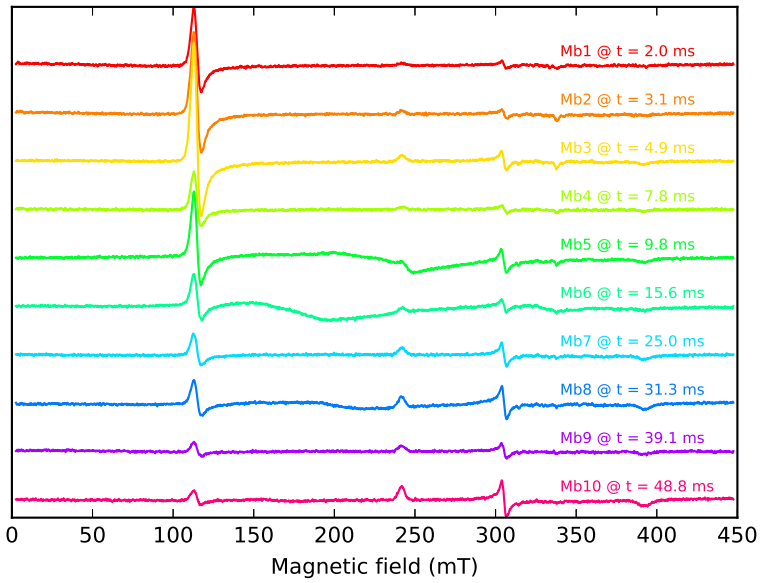

Figure 2.4: Baseline-corrected, single-scan 9.5 GHz cw EPR spectra of RFQ samples, Mb1 to Mb10, in the time range between 2.0 and 48.8 ms.

range of the contamination.
From the logarithmic linearization of the decay (Figure 2.5, bottom) the apparent reaction rate $k' = 50 \pm 3$ ms^{-1} is extracted by use of Equation 2.2. The k' then yields the real reaction rate $k = 4.2 \pm 0.2 \cdot 10^3$ M^{-1} s^{-1} through Equation 2.3. By extrapolating the semilogarithmic line to $\ln Y(t) = 0$, a freezing time of 7.9 $\pm$ 0.4 ms is obtained.

Figure 2.6 shows the 275 GHz spectra of the Mb0 sample to illustrate the low-field HS-Fe(III) signal at $B_0 = 3.54$ T (left), and the Mn^{2+} signal (right) around $g = 2$ (central $B_0 = 9.8453$ T). Because the range of the magnetic field is broad, it is more convenient to record the two spectra separately. The six lines of the manganese spectrum arise from the transition between the two spin states $m_s = \pm 1/2$, which are further split by the hyperfine interaction with the $I = 5/2$ nuclear spin of Mn.

Figure 2.7 shows the Mn^{2+}-normalized spectra of the RFQ samples Mb1 to Mb10. The solution Mb0 is included to show the intensity of the HS-Fe(III) signal in the absence of sodium azide, i.e., ideally at a reaction time $t = 0$. The decay of the HS-Fe(III) signal as a function of time, obtained from the spectra of the RFQ samples Mb1 to Mb10, is depicted in Figure

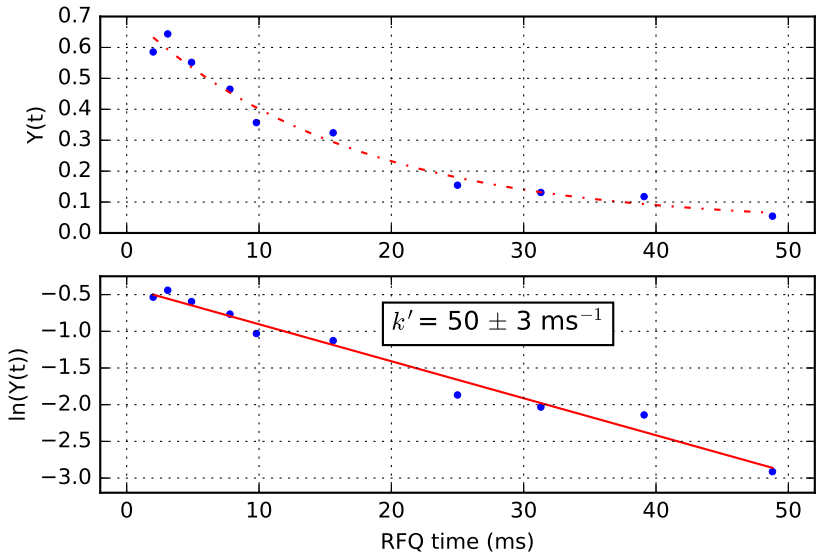

Figure 2.5: $Y(t)$ (top) and $\ln Y(t)$ (bottom) as a function of the calculated reaction time, obtained from the baseline-corrected spectra at 9.5 GHz. The red dashed curve in the top graph is a guide to the eye, while the red line in the bottom graph is the linear regression of the data points.

2.8 (top), along with the linearization of the points. The HS signal intensity was taken at $B_0 = 3.4780$ T (max) and $B_0 = 3.5948$ T (min), while the Mn^{2+} intensity was taken from the sixth peak of the Mn^{2+} spectrum at $B_0 = 9.8680$ T (max) and $B_0 = 9.8690$ T (min).

An apparent reaction rate $k' = 52 \pm 2$ ms^{-1} is extracted with Equation 2.2, from which the reaction rate $k = 4.3 \pm 0.2 \cdot 10^3$ M^{-1} s^{-1} is obtained with Equation 2.3. By extrapolating the semilogarithmic line to $\ln Y(t) = 0$, a value of 0.25 $\pm$ 0.01 ms is obtained.

2.4 Discussion and conclusions

The reaction rates calculated from the logarithmic $Y(t)$ curves obtained from 9.5 GHz and 275 GHz spectra (Figures 2.5 and 2.8, respectively) coincide, keeping into account the measurement errors of about 4 and 6 %, respectively.

As mentioned in the Results Section, by extrapolating to $\ln Y(t) = 0$ of the semilogarithmic lines of the decays obtained at 9.5 and 275 GHz, values of 7.9 $\pm$ 0.4 ms and 0.25 $\pm$ 0.01 ms are

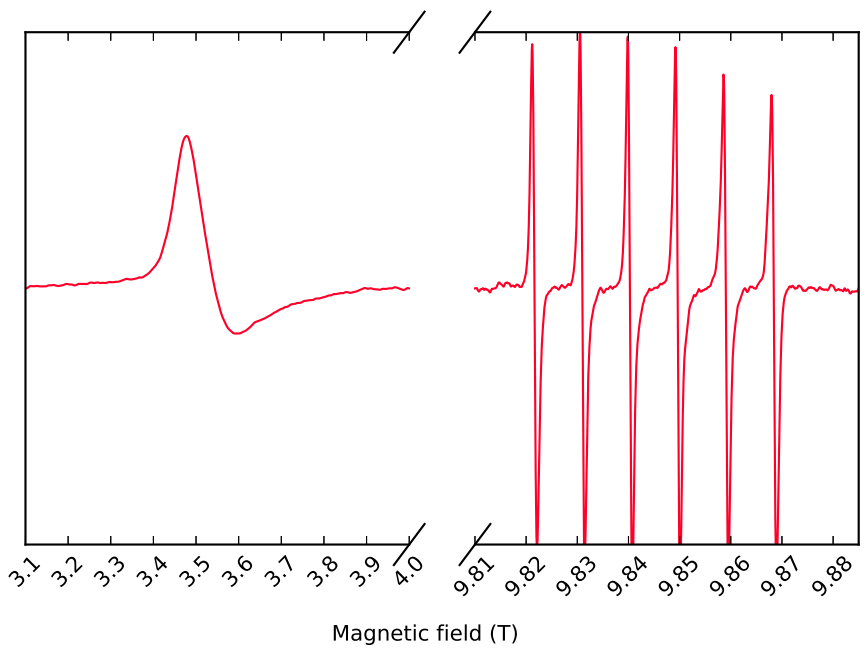

Figure 2.6: Baseline-corrected, averaged 275 GHz spectra of sample Mb0: the myoglobin HS-Fe(III) signal (left), and the Mn^{2+} signal (right).

obtained, respectively. While for the experiments at 9.5 GHz the Mb0 sample (representing the reaction at $t = 0$) was prepared from the very same solution batches as the other RFQ samples, for the experiments at 275 GHz this was not possible because, as mentioned in Subsection 2.2.2, these were performed about a year later. The Mb0 solution was thus prepared from different batch solutions than the original ones used to prepare the RFQ samples. It is thus clear that in the case of the experiments at 275 GHz, the Mb0 does not constitute a reliable representation of the reaction at $t = 0$. Therefore, only the semilogarithmic decay obtained at 9.5 GHz can yield a measure of the so-called *freezing time*.

It is interesting to analyze the semilogarithmic decays obtained at 9.5 GHz and 275 GHz *together*, so as to get an average value of k. However, since the semilogarithmic decay at 275 GHz returns a different time when extrapolated to $\ln Y(t) = 0$ than the decay at 9.5 GHz, in order to be able to plot the two together it is necessary to vertically shift the former by a factor ΔY given by 2.9:

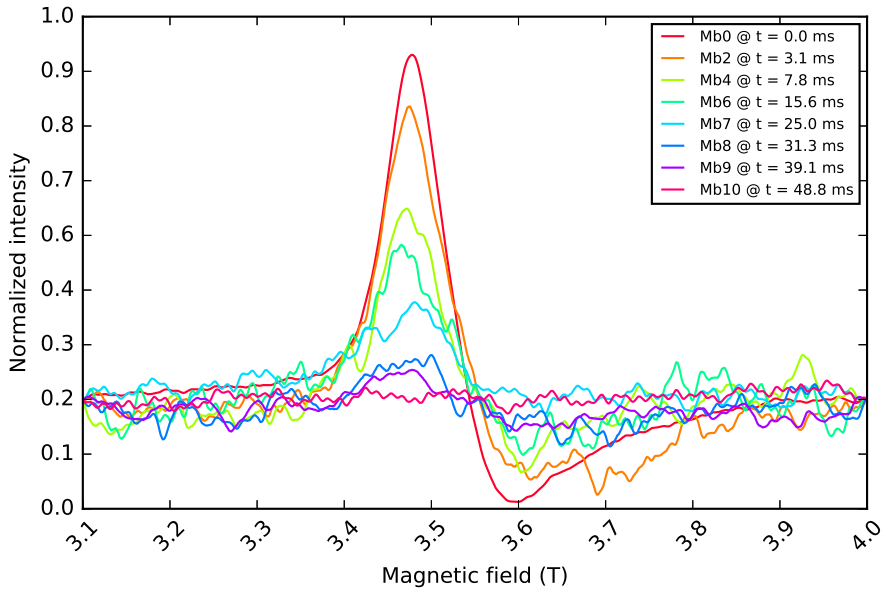

Figure 2.7: Baseline-corrected, Mn^{2+}-normalized, averaged 275 GHz spectra of RFQ samples Mb2, Mb4, Mb6, Mb7, Mb8, Mb9, and Mb10. Sample Mb0, which concerns the $t = 0$ solution without sodium azide, is also included.

$$\Delta Y = \frac{m_{275}}{m_{9.5}} q_{9.5} - q_{275} = 0.4 \tag{2.9}$$

where m_{275}, $m_{9.5}$, and q_{275}, $q_{9.5}$ indicate respectively the slopes and intercepts of the linear fits of the logarithmic $Y(t)$ curves, from 275 and 9.5 GHz experiments.
If the points of the 275 GHz kinetics are thus shifted by ΔY, as expected they end up within the same range as the points of the 9.5 GHz kinetics, and in this way it is possible to calculate a regression line originating from the unified points at 9.5 and 275 GHz (Figure 2.9). An apparent k' is thus obtained of 51 $\pm$ 2 ms^{-1} by use of Equation 2.2, corresponding to a reaction rate $k = 4.2 \pm 0.2 \cdot$ M^{-1} s^{-1} (obtained through Equation 2.3).

As summarized in Table 2.4, this value of k lies in the range of reaction rates to be found in the literature for the myoglobin-azide reaction, under conditions similar to those of the present work. It should be noticed that the reaction has a critical dependence on the pH [45] and on the azide concentration [35] [36], although in theory all the studies reported in Table 2.4 are carried

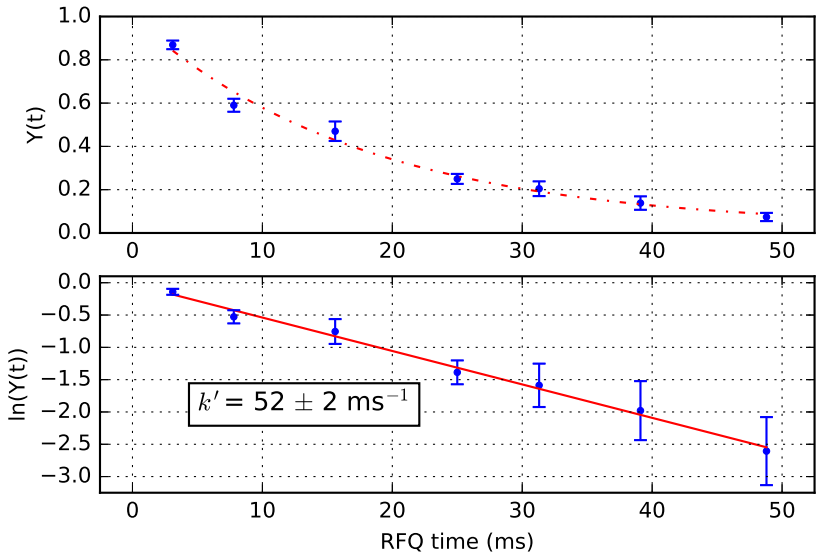

Figure 2.8: $Y(t)$ (top) and $\ln Y(t)$ (bottom) as a function of the calculated reaction time, obtained from the spectra at 275 GHz. The red dashed curve in the top graph is a guide to the eye, while the red line in the bottom graph is the linear regression of the data points.

out under pseudo-first-order conditions. Given these considerations, the k found in the present work is in good agreement with the data from the literature.

In conclusion, these results convincingly prove that the method described in the present work, i.e., the coupling of RFQ to HF-EPR, is successful.
The approach is based on a previously developed method that enables the efficient and reproducible packing of RFQ samples in 150-μm sized capillaries suitable for 275 GHz EPR, and the safe and fast loading of the capillaries in the pre-cooled cryostat of our 275 GHz EPR spectrometer.
Besides this notable improvement over other methods reported in the literature so far, our approach also allows the use of only one single series of RFQ samples, to be used both at 9.5 and 275 GHz, and flexibly at any intermediate frequency in between. This remarkable advantage reduces the amount of material to be used in kinetic studies (which is particularly beneficial for biological samples), and improves the consistency of the method in that only one set of samples is used for the two frequencies.

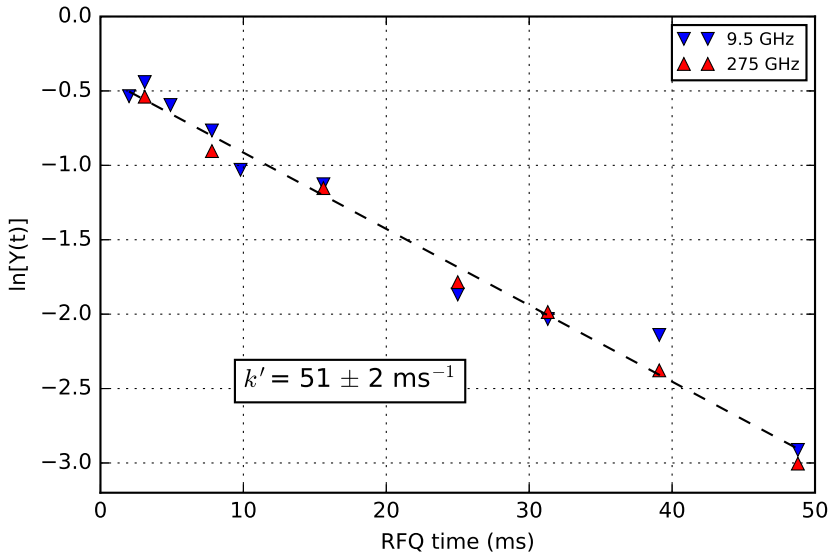

Figure 2.9: Logarithmic plots of $Y(t)$ from 9.5 and 275 GHz spectra. The dashed line is a regression obtained from analyzing the two kinetics together, after shifting the points from 275 GHz by the amount ΔY.

Source	k ($\cdot 10^3$ M^{-1} s^{-1})	[metMb] : [Az] (mM)	pH	T (°C)
This work	4.2 $\pm$ 0.2	1.2 : 12	7.8	21.5
[45]	4.4 / 3.1 / 2.5	0.09 : 0.05 $\div$ 0.7	7.0 / 7.3 / 7.5	25.0
[35]	3.04 (2.83)	0.44 : 6.25 (12.5)	7.8	21.7
[36]	2.9 (1.9)	0.25 : 6.25 (12.5)	7.8	21.8
[39]	2.2	0.625 : 6.25	7.8	22.0
[21]	6.0	1 : 5	7.0	23.0
[37]	2.8 $\pm$ 0.3	2.4 : 30	7.8	not specified

Table 2.4: Comparison of the values of k for the reaction of metmyoglobin (metMb) with sodium azide (Az), as found in the present work and from the literature, under similar conditions of concentration ratios, pH, and temperature. In References [35] and [36], two different values of k are found for two different concentrations of sodium azide, which are reported in brackets. In Reference [45], three different values of k are found for three different values of pH; as far as the concentration of sodium azide is concerned, the authors refer to a range of concentrations, without specifying the actual ones.